PERGAMON

Journal of Structural Geology 24 (2002) 709–727

JOURNAL OF STRUCTURAL GEOLOGY

www.elsevier.nl/locate/jstrugeo

Relay zones between mesoscopic thrust faults in layered sedimentary sequences

Andrew Nicol[a,b], Paul A. Gillespie[a,c], Conrad Childs[a,d,*], John J. Walsh[a,d]

[a]*Fault Analysis Group, Department of Earth Sciences, University of Liverpool, Liverpool L69 3GP, UK*
[b]*Institute of Geological and Nuclear Sciences, PO Box 30368, Lower Hutt, New Zealand*
[c]*Norsk Hydro ASA, Sandsliveien 90, N-5020 Bergen, Norway*
[d]*Fault Analysis Group, Department of Geology, University College Dublin, Belfield, Dublin 4, Ireland*

Received 4 August 2000; revised 7 February 2001; accepted 30 April 2001

Abstract

We examine the geometry, formation and destruction of relay zones in well-bedded sedimentary sequences containing thrust fault segments with maximum observed displacements of 0.64–8 m. Contractional, extensional and neutral relay zones are distinguished based on the stepping sense of the interacting fault segments and the orientation of the associated fault slip vectors. Large displacement gradients (0.17–1.0) in relay zones are mainly accommodated by folding with aggregate displacements maintained across segment boundaries and a significant component of the fault slip converted to fold-related shortening.

Folds in contractional relay zones verge in the direction of hanging wall motion, with the steeper limb defining a parallelogram-shaped zone between thrusts. Fault segment lengths are established after minimal displacement and folds in relay zones grow between segments as displacement accrues on the thrusts. With increasing displacement, upper and lower thrust tip lines in contractional and extensional relay zones are fixed at stratigraphic boundaries while the lateral thrust tip lines may propagate in a strike-parallel direction. Upper and lower tip lines may eventually propagate to bypass relay zones that formed early in the fault growth history. Contractional relay zones remain intact at higher displacements than extensional relay zones.

Keywords: Relay zones; Mesoscopic thrust faults; Layered sedimentary sequences

1. Introduction

Segmented fault traces are seen over a large range of scales (Griffiths, 1980; Larsen, 1988; Peacock and Sanderson, 1991, 1994; Stewart and Hancock, 1991) and occur in all modes of faulting (Aydin, 1988; Walsh et al., 1999). Regions near fault tip lines and between adjacent fault segments are often zones of concentrated strain associated with the loss of displacement on individual faults (e.g. Elliott, 1976) and the transfer of displacement between fault segments (e.g. Dahlstrom, 1969; Gardner and Spang, 1973). If a fault tip line is pinned, increasing displacement results in an increase in strain in the region surrounding the fault tip line. In the case of a relay zone between faults, when the strain reaches some critical value, the faults propagate across the relay zone and a throughgoing fault surface forms. Such fault segment linkage is recognized as one of the most important processes in the growth of fault systems (Dahlstrom, 1969; Peacock and Sanderson, 1991; Cartwright et al., 1995; Childs et al., 1995; Ferril et al., 1999; Gupta and Scholz, 2000).

The zone of displacement transfer between en échelon fault segments has been variously referred to as a jog, step-over, relay zone, fault bridge, transfer zone and relay structure. The established term in the thrust literature is 'transfer zone' (Dahlstrom, 1969), however, as many of the comments in the opening sections of this article are not specific to thrust faults, here we use the term 'relay zone', which has been applied to each mode of faulting (Walsh et al., 1999).

Faults may be segmented vertically or laterally and the interaction of adjacent fault segments can be classified according to the relative orientations of the fault segment boundaries and their associated slip vectors (Fig. 1; Peacock and Sanderson, 1991). For vertically-segmented dip-slip faults, the axis of the fault segment boundary is horizontal and normal to the fault slip direction. Depending on the

* Corresponding author. Correspondence address: Fault Analysis Group, Department of Geology, University College Dublin, Belfield, Dublin 4, Ireland. Tel.: +353-1-706-2606; fax: +353-1-706-2607.
E-mail address: conrad@fag.ucd.ie (C. Childs).

0191-8141/02/$ - see front matter
PII: S0191-8141(01)00113-4

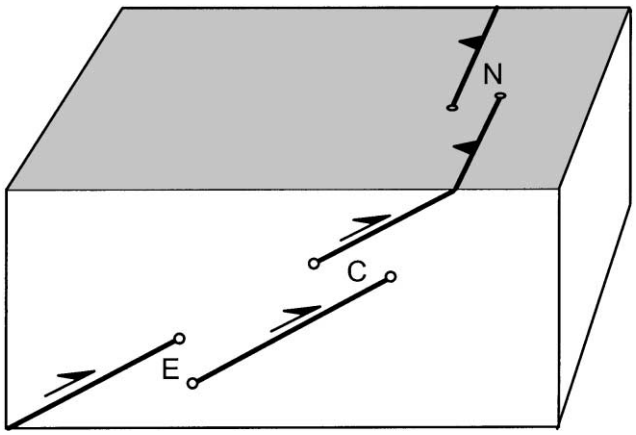

Fig. 1. Block diagram illustrating contractional (C), extensional (E) and neutral (N) relay zones between thrusts.

sense of stepping of the fault segments, relay zones between such vertically-segmented faults will be regions of contractional or extensional strain (Fig. 1). For laterally-segmented dip-slip faults the axis of segmentation parallels the fault slip direction. In this case the transfer of displacement between fault segments is effected by simple shear not requiring volumetric strains.

Walsh et al. (1999) suggested that contractional, extensional and neutral relay zones occur in each mode of faulting and that the internal structure of a relay zone is largely dependent on the relative orientations of the fault segments and the lithological layering. Although each of the three types of relay zone have been well described in normal fault systems (e.g. Larsen, 1988; Morley et al., 1990; Peacock and Sanderson, 1991, 1994; Walsh and Watterson, 1991; Peacock and Zhang, 1994; Trudgill and Cartwright, 1994; Childs et al., 1995; Huggins et al., 1995), extensional

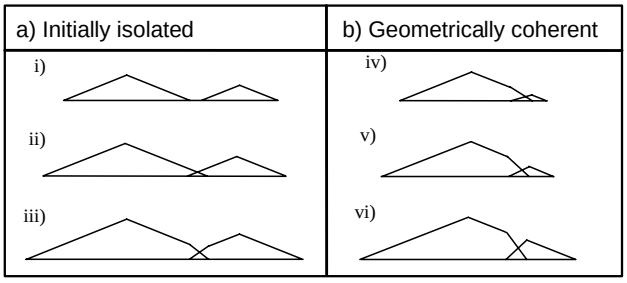

Fig. 2. Schematic illustration of the evolution of displacement distance profiles as displacement accrues on pairs of sub-parallel, non-colinear faults. Where the faults are initially isolated from one another they (i) propagate towards each other to overlap, and (ii) eventually interact resulting in (iii) high lateral displacement gradients within a relay zone. Where the faults are geometrically coherent from the outset (iv) a relay zone is already established. Continued accumulation of displacement causes a progressive increase in gradient within the relay zone (v and vi). The aggregate displacement profile (not shown) in each of the two cases differs in that the points of maximum displacement are preserved where the faults were initially isolated but a simple aggregate profile occurs at all stages of development of the geometrically coherent faults. The displacement profiles can apply to either the strike or dip directions.

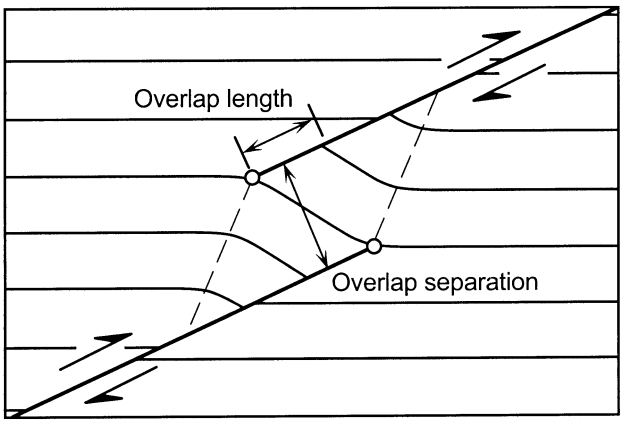

Fig. 3. Schematic diagram illustrating thrust trace and associated fold geometries in cross-section for a relay zone in a well-bedded sequence. Use of the terms overlap separation and overlap length is shown. Thrust segments that underlap have negative overlap lengths.

and contractional relay zones have been described for strike-slip fault systems (e.g. Aydin and Nur, 1985; Woodcock and Fischer, 1986; Wesnousky, 1988; Peacock, 1990), and neutral relay zones have been extensively described for thrust faults (e.g. Dahlstrom, 1969, 1970; Gardner and Spang, 1973; House and Gray, 1982; Liu and Dixon, 1991; Lebel and Mountjoy, 1995), there is significantly less literature describing extensional and contractional relay zones along thrust faults (e.g. Aydin, 1988; McConnell et al., 1997).

As with normal faults, vertical segmentation of thrusts should be enhanced in layered sequences where there are significant differences in rock properties across layer interfaces. In these situations, thrust propagation is impeded at the interfaces between layers and thrust tip lines may become pinned in mechanically weak layers that are adjacent to strong layers.

2. Research scope and methodology

The primary aim of this paper is to describe and analyze several mesoscopic field examples of thrust-related relay zones. Our ultimate purpose is to understand how discontinuous thrust fault segments kinematically interact and eventually link to form a continuous three-dimensional (3D) fault surface. To this end, we analyze in detail the displacement distributions, associated folding and geometries of fault segments that interact across a relay zone. We suggest that the character of fault displacement distributions in relay zones can be used to determine whether adjacent fault segments formed in isolation and grew together, or if they were kinematically linked since their inception (Fig. 2). If the displacements on adjacent fault segments and the continuous strains within a relay zone sum together to form a displacement distribution that is similar to that of a single fault, the fault segments are said to be geometrically

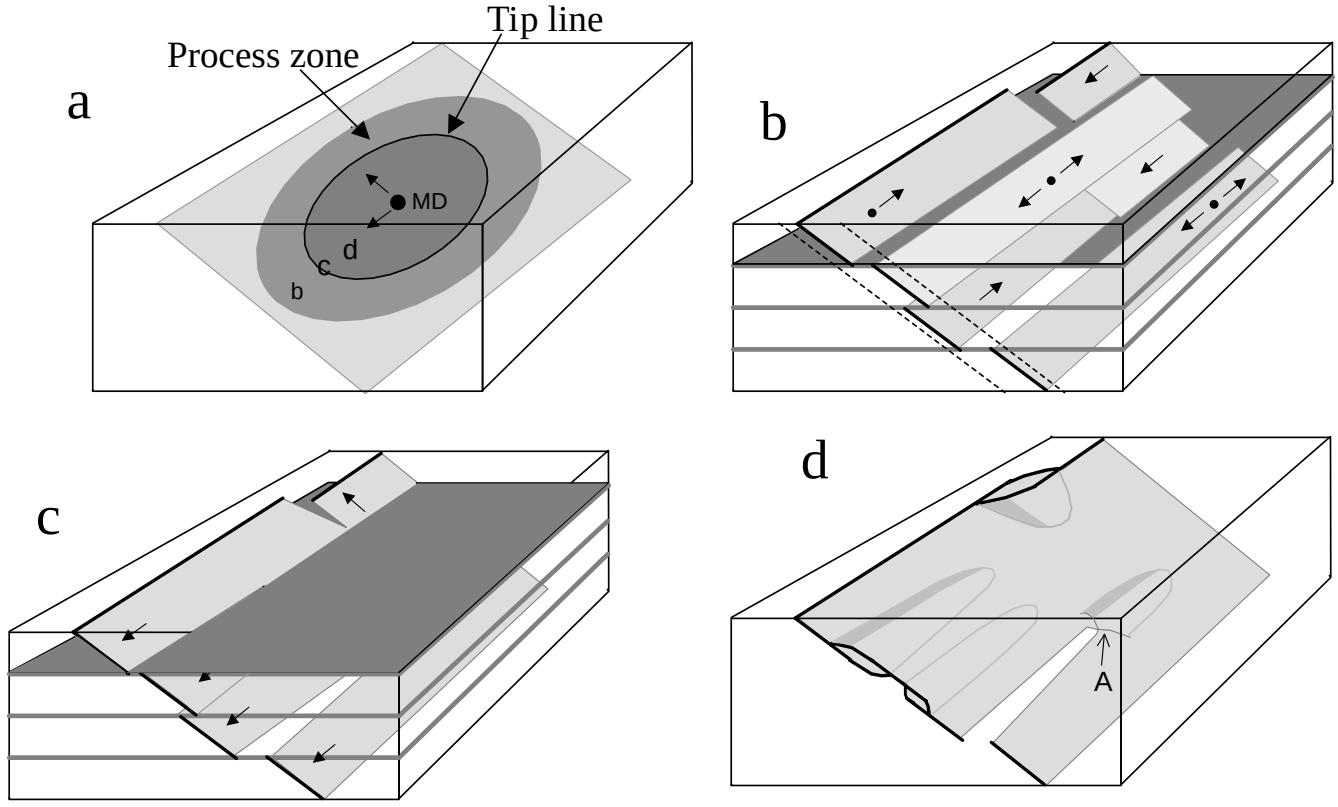

Fig. 4. (a) Cartoon of an elliptical thrust showing the tip line bounding the parent slip surface and the edge of the process zone ahead of the tip line. Arrows indicate fault propagation directions that radiate from the point of maximum displacement (MD) at the centre of the fault. Block diagrams (b,c and d) illustrate the variation in fault zone structure from the process zone to the centre of a thrust surface. (b) Unconnected minor fault segments within the thrust process zone. The upper and lower tip lines of each segment occurs within a relatively incompetent layer (black horizontal lines). Arrows indicate the local propagation direction of each segment. The margins of the process zone are shown with the dashed lines. (c) The fault zone geometry within, but proximal to, the tip line showing lateral and vertical bifurcations of the parent thrust surface. (d) The fault zone geometry within and distant from the tip line. The area labelled A indicates part of an extensional relay at the point of breaching.

coherent (Walsh and Watterson, 1991). Pairs of faults that are geometrically coherent are interpreted to have been active at the same time and were kinematically linked since their inception (see next section). If they were initially isolated, faults bounding a relay zone will have a displacement distribution with a deficit between the displacement maxima of the two adjacent faults. The magnitude and geographic extent of this displacement deficit will vary depending on when the two faults began to interact and thereafter became kinematically linked.

Large displacement gradients in relay zones in well-bedded sequences are generally accommodated by bed rotations (Morley et al., 1990; Peacock and Sanderson, 1991, 1994; Anders and Schlische, 1994; Trudgill and Cartwright, 1994; Childs et al., 1995, 1996a; Huggins et al., 1995). Fig. 3 illustrates the idealized cross-sectional geometry of a contractional relay zone between two thrust segments in well-bedded sedimentary rocks. The geometry of such relay zones is variable and depends upon a number of factors that include overlap length and separation, thrust displacement, mechanical unit thicknesses relative to overlap separation and the mechanical properties of the sedimentary sequence. Because these factors may be spatially variable over a single fault surface, individual relay zones will vary in geometry depending on where they develop along a fault surface. Despite this inherent variability, however, contractional relay zones contain generally similar styles of folding.

We are not concerned here with the strains that occur at the free tips of propagating faults, but only those strains that result from interaction between coeval thrusts. We do however suggest that the thrust relay zones described here could be misinterpreted as tip line folds and that thrust relay zones are more common than the literature would suggest. Thrust relay zones and tip line folds should be distinguishable from differences in bed geometry (Fig. 3) and fault displacement distribution (Fig. 2; see Section 5.1).

3. Conceptual model

A conceptual model illustrating the role of relay zones in the growth of a thrust fault in a layered sequence is illustrated in Fig. 4. The model fault is elliptical, elongate in the strike dimension (aspect ratio = 2) and propagates radially from the point of maximum displacement at the centre of the

Table 1
Geometries and displacements of thrust relay zones together with details of locations and sequences of examples presented in this paper

Name	Location	Sequence	Relay type	Overlap separation (m)	Overlap length (m)[a]	Max. displ. (m)[b]	Data source
Nant Helen opencast	South Wales, UK	Fissile mudstones Westphalian age	Contractional	2.4	− 1.2	8.0 7.0	Gillespie (1991)
Black Rock Quarry[c] Example 1	Clydach Gorge, South Wales, UK	Well bedded Carbonif. limestone & marls	Contractional	2.9–6	9.2	3.8 6.0	Gillespie (1991)
Eagle Rock	Western Virginia, USA	Well bedded Silurian sandstone & shale	Contractional	0.6–0.8	1.05	0.87 0.97	McConnell et al. (1997)
Broadhaven 1	Pembrokeshire, South Wales, UK	Well bedded Carbonif. mudstone & siltstone	Contractional	0.7	1.0	0.64 1.14	This study & Gillespie (1991)
Broadhaven 2	Pembrokeshire, South Wales, UK	Well bedded Carbonif. mudstone & siltstone	Neutral	0.75	− 2.5	0.74 0.99	This study
Whakataki	Wairarapa, North Island, NZ	Well bedded Miocene mudstone & siltstone	Extensional	5.0	− 3.0	1.62 1.33	This study

[a] Positive numbers indicate overlap and negative values underlap (see Scholz 1990, p. 148).
[b] Top and bottom displacements refer to upper and lower thrusts.
[c] Includes data from south wall of quarry.

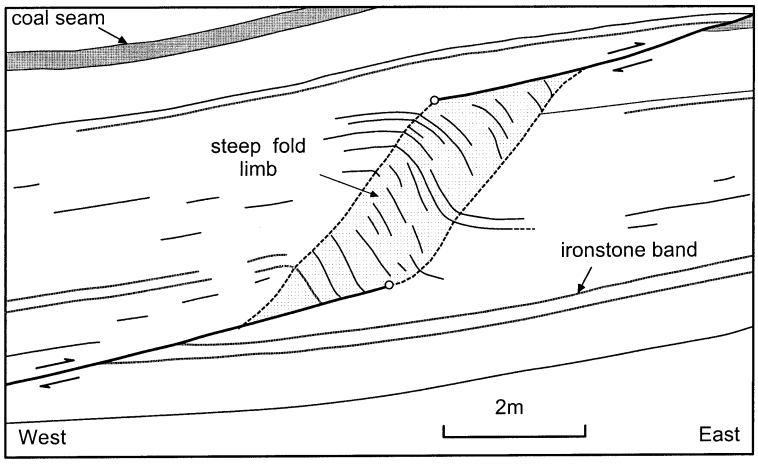

Fig. 5. Cross-section of a monoclinal fold between the tip-points of two shallow dipping (25°) thrust traces, in fissile mudstones of Westphalian age (after Gillespie, 1991). The cross-section is oriented at ~50° to fault strike. Broken lines and shading define the steep limb of the fold.

fault. Ahead of the propagating tip line of the parent thrust surface, minor unconnected faults nucleate within the process zone (Fig. 4b). Although the process zone as a whole propagates radially (Fig. 4a), individual fault segments within the process zone propagate from their independent nucleation points and may interact with one another or the parent fault to form relay zones. The parent fault surface advances both by linking with, or capturing, minor faults formed in the process zone and by propagating through unfaulted rock. In the latter case, the parent fault bifurcates due to mechanical heterogeneity of the sequence (Fig. 4c). Both bifurcation and the capture of initially unconnected fault segments results in a highly irregular fault tip line with re-entrants occurring on a range scale. These re-entrants are fault segment boundaries which, as displacement accrues, become sites of displacement transfer and relay zone formation. In mechanically layered sequences, fault propagation is arrested in the more ductile units so that tip line re-entrants and therefore relay zones will preferentially form at weaker layers. As displacement accrues, strain within a relay zone increases until it is breached and bypassed by the formation of a throughgoing fault (Fig. 4d). Areas of the fault surface distant from the tip line are populated with breached relay zones on a variety of scales. The preservation potential of unbreached, or intact, relay zones depends largely on the overlap separation (Childs et al., 1996b), so that larger separation relay zones are expected to remain intact closer to the centre of the fault surface than those with small separations (Fig. 4d).

This model illustrates the spatial variation in fault zone structure over a thrust surface but can equally represent the temporal variation in structure at a point on the thrust. When this point lies at the centre of the fault then Fig. 4b represents the fault zone structure at the time of fault initiation and prior to development of the parent fault surface.

In this model all of the individual fault segments, whether they initiated in the fault process zone or due to bifurcation of the parent fault tip line are, from their time of formation, part of a single geometrically coherent structure. Segmented fault trace cross-sections through the conceptual fault zone represent either unconnected fault segments within the process zone (Fig. 4b) or connected fault segments in the tip region (Fig. 4c).

4. Geometry of relay zones

We present six examples of segmented fault traces (Table 1) from outcrops of well-bedded Miocene (New Zealand) and Paleozoic sequences (Appalachians, USA and South Wales, UK), that were observed partly or entirely in sections normal to the strike of bedding. The segment boundaries are contractional (Figs. 5–10), extensional (Fig. 11) or neutral (Fig. 12) with folding or bed rotations present between the component fault segments. Calcite fibres and slickenside striations or grooves indicate that faults are dip-slip (Figs. 6 and 8–10), with movement within ~20° of the fault dip direction. The faults have maximum displacements of 0.64–8 m (Table 1) and trace lengths greater than 20 m. The faulted sequences are well-bedded and comprise interbedded mudstone and sandstone or limestone with mechanical unit thicknesses at relay zones typically <10% of the overlap separation (see Fig. 3 for terminology).

Displacement-distance plots (Muraoka and Kamata, 1983; Williams and Chapman, 1983; Chapman and Williams, 1984; Barnett et al., 1987; Ellis and Dunlap, 1988; Peacock, 1991; Hedlund, 1997; McConnell et al., 1997) have been used to assess the kinematic relationships between faulting and folding across segment boundaries. Bedding surface offsets were measured for thrust segments in four cases and include heave (Fig. 6), displacement along the fault between horizon cutoffs (Figs. 7, 11 and 12) and throw (Fig. 8). In Figs. 6 and 8 these measurements allow comparison between fault and fold displacements across the relay zones. Fold displacements were estimated by

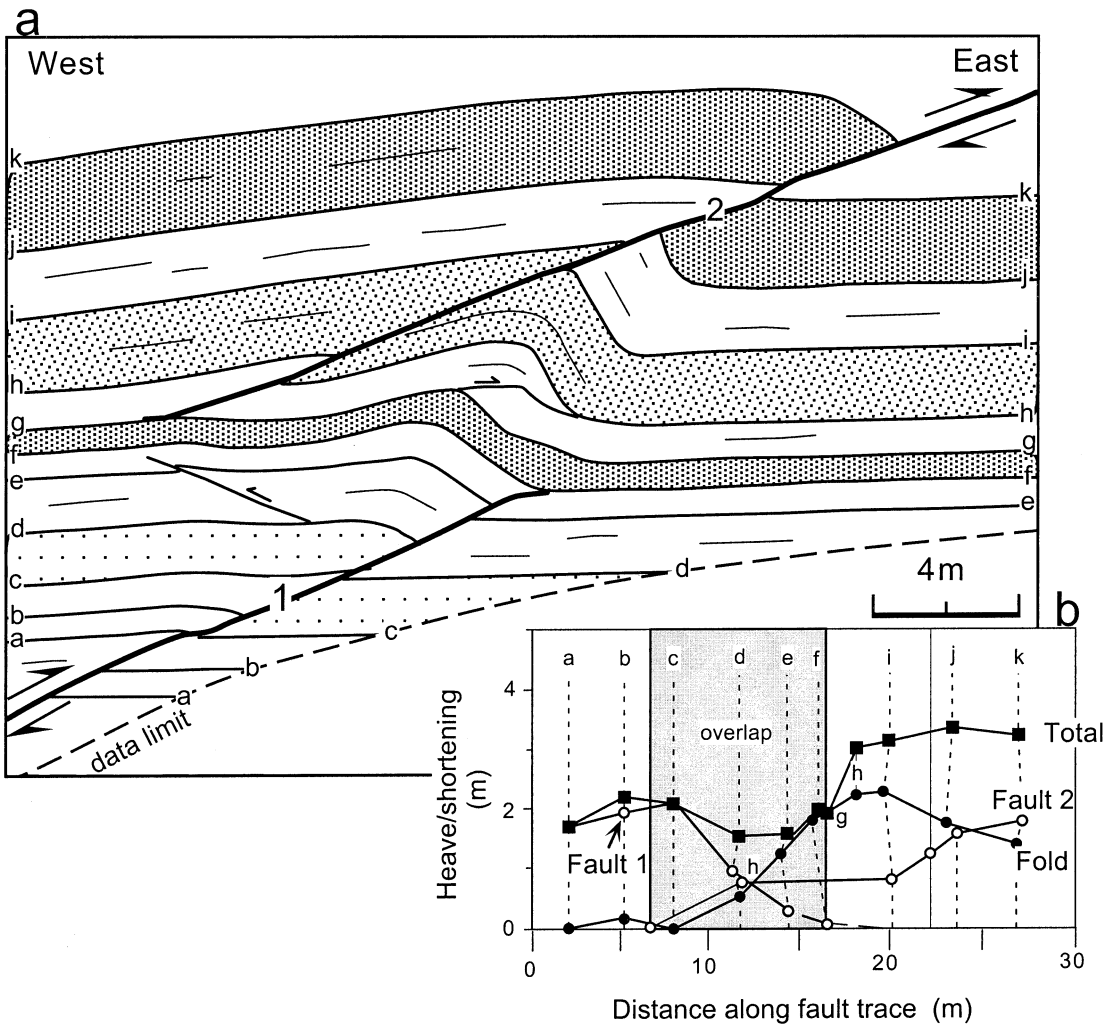

Fig. 6. Cross-section (a) and displacement profiles (b) for two overlapping thrust segments (labelled 1 and 2), which dip at 22–27° and are separated by an asymmetric fold within well-bedded Carboniferous limestone (bed thicknesses 0.1–1 m) and marl beds (thicknesses 0.01–0.3 m) at Black Rock Quarry, Clydach Gorge, South Wales (cross-section modified from Gillespie (1991) and Hathaway and Gayer (1996)). The cross-section is oriented at ~75° to fault strike. Limestone beds are shaded to aid visualisation. Heaves on the thrust segments and the fold shortening were measured parallel to the thrust dip direction at outcrop. Heave, fold shortening and total shortening were measured from bedding surfaces and are plotted against distance from the base of the outcrop along a line parallel to fault dip. On the displacement profile, values are plotted at the mid points of each of the displaced horizons; as folding of each horizon occurs in the footwall and hanging wall of both thrust segments, the fold and aggregate mid points are coincident. Displacement measurements are less reliable along the upper thrust as this part of the outcrop is irregular and largely inaccessible.

measuring shortening due to bed rotations (Fig. 6) and by calculating the difference between fault throw and total vertical separation on individual beds (Figs. 8 and 11).

4.1. Contractional relay zones

The segmented thrusts in Figs. 5–10 exhibit contractional relay zones (Table 1), that trend at a high angle to fault slip (>60°) and that were observed in cross-section (Figs. 5–7 and 10) or in both cross-section and map view (Fig. 8). The general form of the structures in Figs. 5–8 is similar, despite differences in the scale, detailed geometry (e.g. displacements, overlap length and separation) and lithological sequence (Table 1). In each case thrust segments inclined at low angles to regional bedding (cutoff angles ~10–25°) are separated by an asymmetric fold, with steep to moderate bed dips of ~30–75° within the relay zone and shallow bed dips outside the relay zone. Folds verge in the direction of hanging wall motion, with the steeper limb of the fold defining a parallelogram-shaped region between thrusts. High bedding cutoff angles between fault segments (typically 60–80°) are not matched by cutoffs external to the relay zone (i.e. in the footwall of the lower thrust and the hanging wall of the upper thrust), which, together with other features (see Section 5.1), indicates that folding post-dates formation of the thrust segments. Commonly, although not exclusively, the synclinal axial trace terminates at the tip-point of the lower thrust, with the steeper fold limb occupying a portion of the total area between the faults (i.e. overlap length × overlap separation). Fold axes trend parallel to

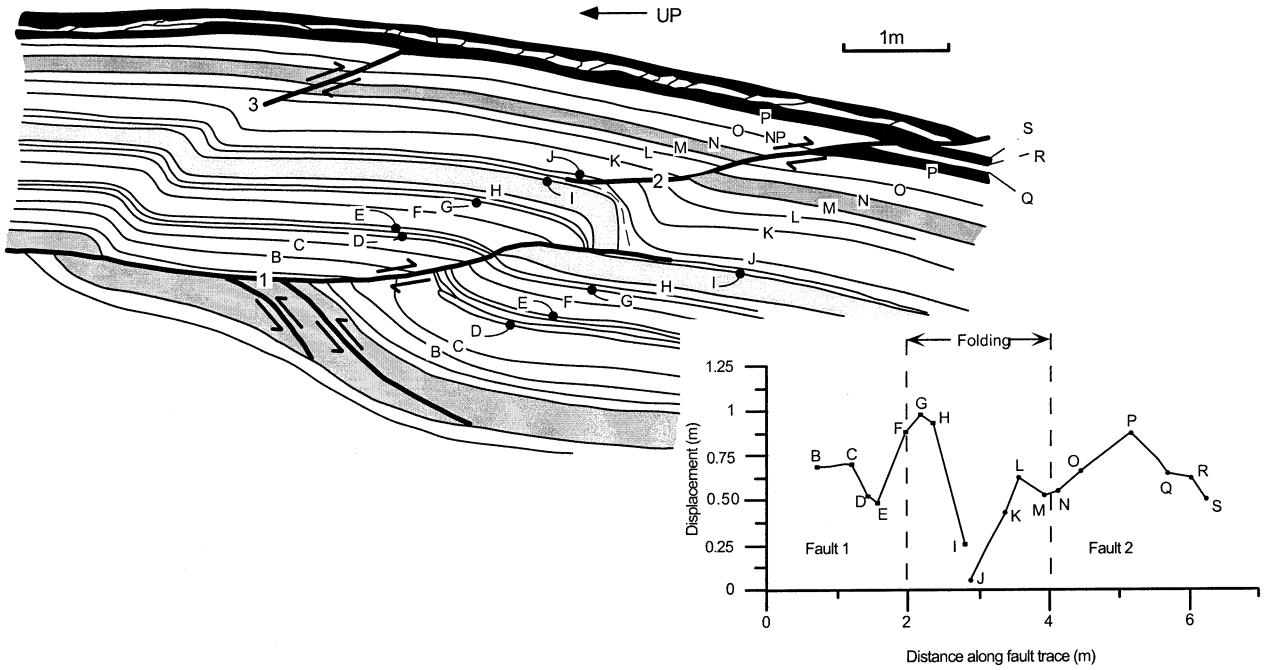

Fig. 7. Cross-section and displacement profiles for two thrust segments and associated fold from a roadcut near Eagle Rock, western Virginia, USA (modified from McConnell et al. (1997)). These structures, previously described by Kattenhorn and McConnell (1994) and McConnell et al. (1997), occur within steeply dipping and overturned Silurian sandstone and shale sequence. The line drawing is rotated so that bedding is horizontal. Distance on the displacement profile is measured along a line parallel to the average thrust orientation.

thrust strike and approximately normal to the fault-slip direction (e.g. Fig. 8). Figs. 6 and 7 differ from the other examples in that the thrusts become bedding-parallel at their tips, with ~10–20% of the total thrust displacement taken up by bedding-plane slip.

Displacement-distance diagrams (Figs. 6–8) show a rapid decrease in thrust displacement within the relay zones (dip-slip displacement gradients of ~0.17–1.0), which is mirrored by an increase in fold amplitude. The region of greatest fold amplitude, or shortening, coincides approximately with a low in thrust displacements (Figs. 6–8). High displacement gradients within the relay zones are accommodated mainly by bed rotations reflecting the transfer of fault slip to folding. Aggregate displacement profiles, incorporating both the thrust and fold-related displacement components, are less variable than either of the components indicating that the thrusts and fold together represent a single coherent structure with discontinuous (i.e. two thrust segments) and continuous (i.e. fold) components of deformation.

Folding between thrust segments is accommodated by a combination of bed-over-bed slip, small-scale thrusts and duplexes, and pressure solution cleavage. Abundant slickenside striations and/or calcite fibres trending down dip on bedding surfaces indicate significant flexural-slip folding between thrust segments in Figs. 5, 6 and 8. Bed rotations between thrust segments are mainly accommodated by bedding-plane shear antithetic to the thrusts. At Black Rock Quarry (Fig. 6), bed rotations are also associated with numerous small thrusts and duplexes that accommodate bedding-parallel shortening and thickening of individual beds by up to 100%. Limb length between thrusts therefore decreases with bed rotation; however, the details of this relationship have not been determined. Bedding-parallel shortening at Black Rock Quarry is accompanied by a penetrative pressure-solution cleavage which fans about the fold axial traces. Pressure-solution cleavage and bed thickness increases are most pronounced at fold hinges suggesting that the positions of hinges were fixed relative to the stratigraphy. Thin sections show fossils which cannot be matched across pressure-solution seams and confirm that material has been removed along cleavage surfaces, but do not allow the volume loss to be quantified.

4.1.1. Three-dimensional geometries

Outcrop data provide constraints on the 3D geometry of relay zones at Black Rock Quarry (Figs. 6 and 10) and Broadhaven 1 (Fig. 8). The relay zone from Black Rock Quarry (Fig. 6) also crops out ~70 m to the south on the opposing quarry wall. Here the maximum displacement on the lower thrust is comparable (ca. 5.5 m) with that on the northern face but the average overlap separation is about 50% less, i.e. 2.9 m (Fig. 10). The decrease in overlap separation is accompanied by a tightening of the fold with a ~30° reduction in the interlimb angle. Common to both exposures of the thrust is a ~0.3-m-thick marl bed (between horizons f and g in Fig. 6, and the stippled layer in Fig. 10) that occurs within the relay zone and which, on the northern quarry wall (Fig. 6), contains the thrust tips. The tip-lines of the relay zone bounding faults exposed in the quarry

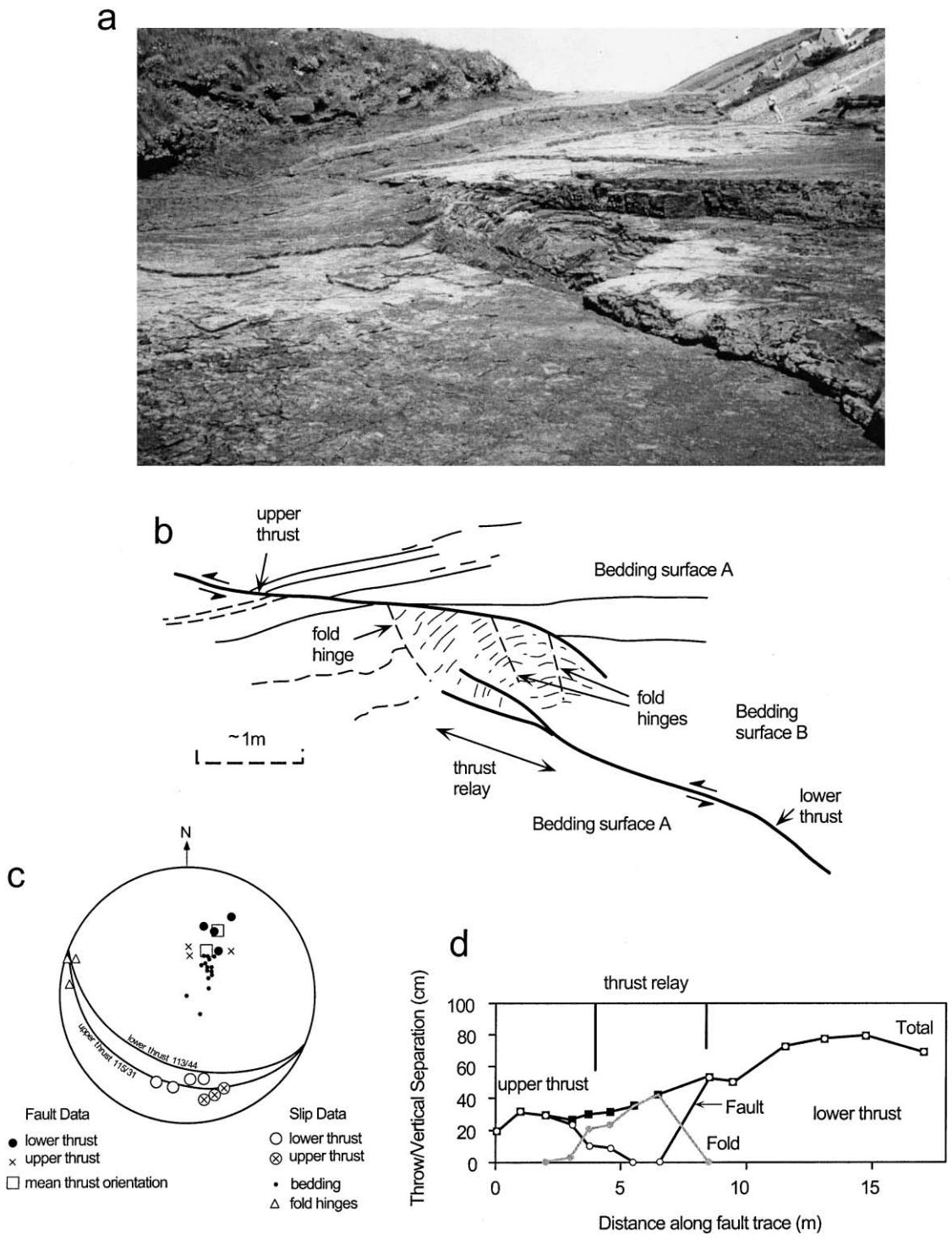

Fig. 8. Segmented Variscan thrust in interbedded Carboniferous sandstones and mudstones, Broadhaven, South Wales, UK. (a) Photograph looking to WNW. (b) Line drawing from photograph. (c) Equal area plot of poles to fault segments, slickenside striations and poles to bedding. (d) Throw/vertical separation profile of the faults, fold and the total vertical separation. Points are plotted as distance along the fault trace at outcrop and all measurements were made at outcrop in the fault slip direction. Referred to as Broadhaven 1 in the text and Table 1. The photograph is rotated so that bedding is horizontal.

are approximately horizontal and parallel to the line of intersection between regional bedding and thrust planes, with their location apparently influenced by the presence of mechanically weak marl beds, as is often the case for segmented normal faults (Peacock and Zhang, 1994; Childs et al., 1996a). Extrapolation of the rate of decrease in the overlap separation observed across the quarry (~4 cm/m) suggests that the two fault segments are likely to be colinear and merge ~70 m beyond the quarry wall to the south (Fig. 10).

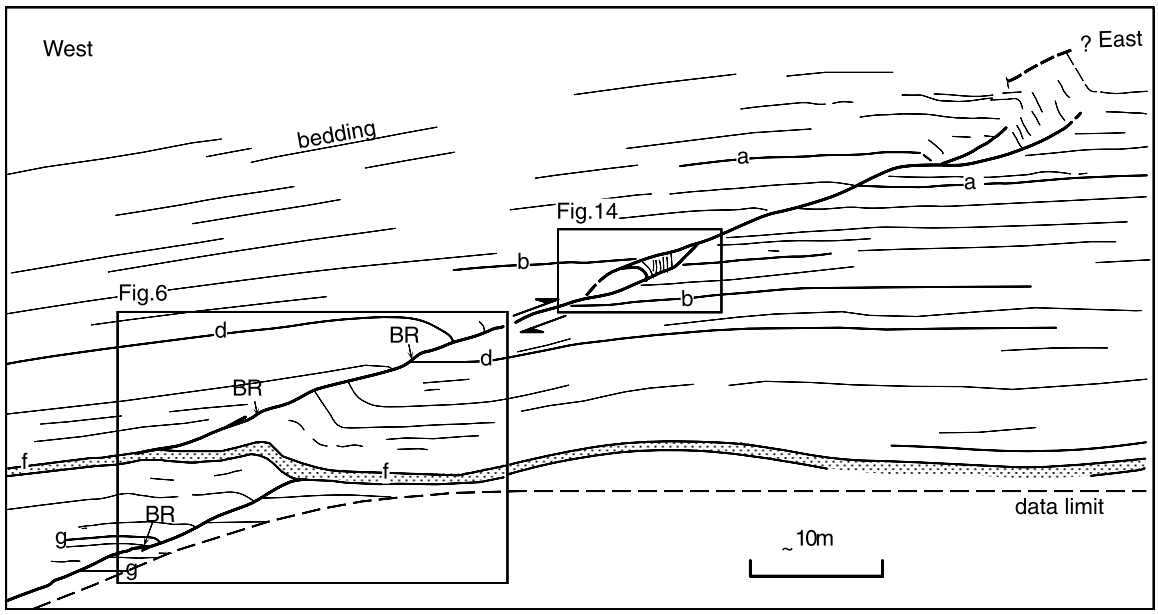

Fig. 9. Thrust at Black Rock Quarry comprising multiple fault segments. The locations of Figs. 6 and 14 are shown. The locations of structures interpreted to be breached relay zones are shown (BR). Selected beds that can be traced across the fault are labelled a, b, d, f and g.

The Broadhaven 1 relay zone and fold in Fig. 8 plunge gently (<10°) to the west (i.e. towards the observer in Fig. 8a and b), again approximately parallel to the line of intersection between regional bedding and the thrust planes. The lateral tip-lines of the thrust segments are, however, not contained within a single vertical plane; instead it appears that the tip-line of the lower thrust extends further west than that of the upper thrust. Thus the relay zone occurs between the upper and lower tip-lines of both thrusts, as is the case for the Black Rock Quarry example, and is also close to the lateral tip-line of the upper thrust. These two examples provide a sample of the type of variability of fault tip-line geometries at relay zones that might be expected for thrusts, but they by no means cover the entire spectrum of possibilities.

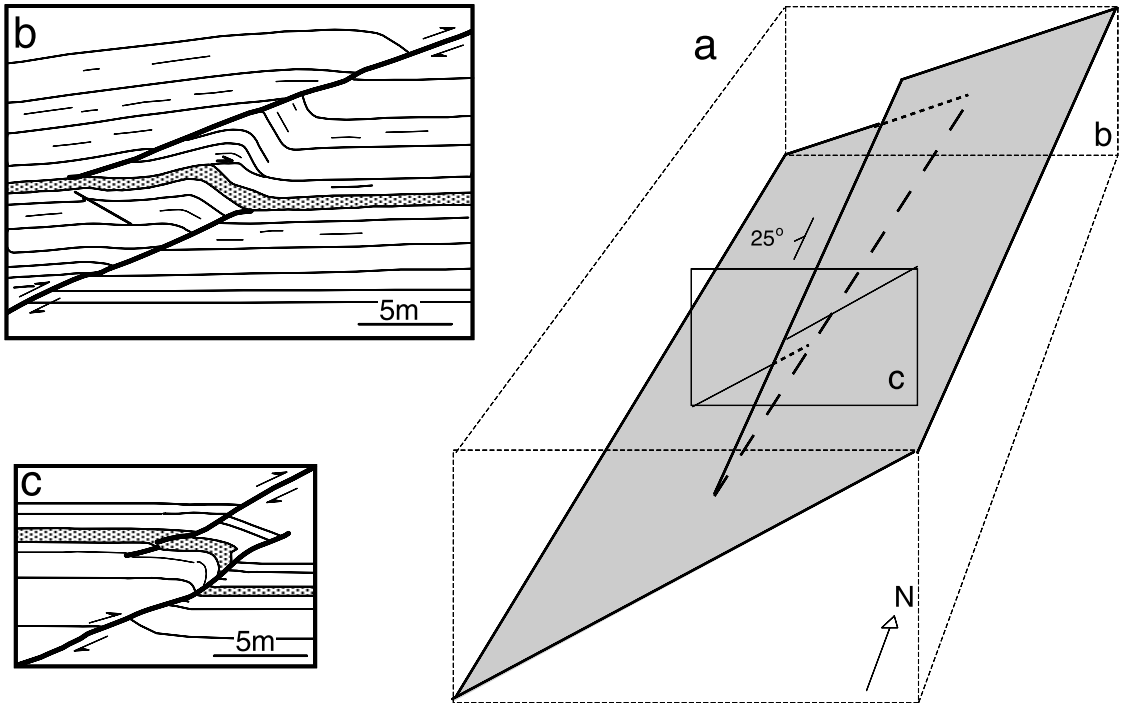

Fig. 10. (a) Schematic diagram showing the relative locations and inferred 3D structure of relay zones exposed on two parallel and vertical quarry walls on (b) the north (Fig. 6) and (c) south sides of Black Rock Quarry.

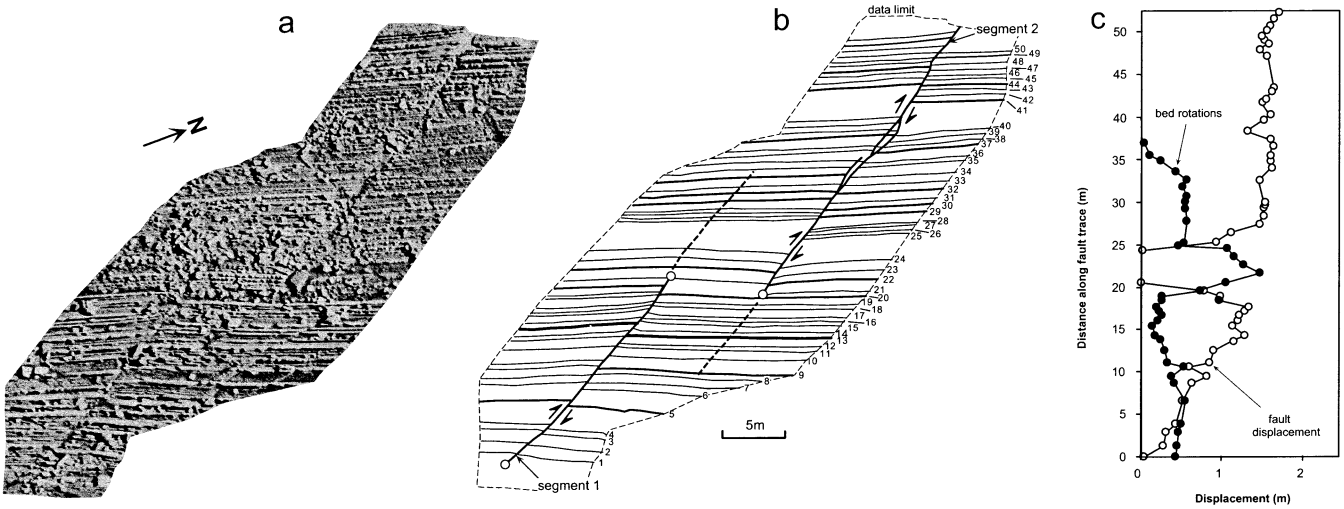

Fig. 11. Segmented fault within a Miocene turbidite sequence from Whakataki, east coast North Island, New Zealand. (a,b) Aerial photograph and map of segmented fault on a horizontal coastal platform. Beds strike at 020–200. (c) Profiles for fault displacement and displacement due to bed rotations (see text for derivation). Distance is measured along a line parallel to the fault traces midway between the two faults. Datapoints for bed rotations are plotted at the intersection between this line and bedding contacts. Displacements were measured in the field parallel to the fault slip vectors. Dashed lines indicate the extent of folding beyond the fault tips.

4.2. Extensional relay zone

An extensional relay zone between strike-slip faults within a well-bedded (bed thicknesses <30 cm and mainly 5–15 cm) turbidite sequence of Miocene sandstones and mudstones from Whakataki, New Zealand is shown in Fig. 11. Beds dip at $\sim55°$ west, fault segments strike at 50–60° to bedding and dip steeply to the north ($\sim70°$), while slickenside and fibre lineations plunge at 16–20° east within 20° of the pole to bedding. Therefore, the segmented strike-slip fault in Fig. 11 has a geometry equivalent to a reverse fault in a horizontally bedded sequence.

Fault segments with displacements ≤1.62 m define a relay zone with an overlap separation of 5 m and underlap of 3 m (Table 1). Within the relay zone, beds are rotated clockwise 6–8° from the regional bed orientation. Beyond the tips of the fault segments, bed rotations initially decrease rapidly but extend at least 10 m from fault tips (Fig. 11c). Bed rotation forms an open antiform west of fault segment 1 and an open synform east of fault segment 2; the width of the zone of rotation is approximately equal to the overlap separation. Displacements accommodated by bed rotations (Fig. 11c) were estimated by extrapolating bed orientations outside the relay zone, across the relay zone to the point of intersection on the opposing fault. The distance along the fault between the actual and projected bed cutoff positions is equal to the displacement taken up by rotation. These values were compared with apparent displacements measured in the plane of the data and directly reflect the geometry of beds within the relay zone. As in contractional relay zones, fault displacements decrease rapidly close to the segment boundary and comparison between fault displacement variations and the displacement accommodated by folding suggests that the fault segments and related folding are components of a single structure (Fig. 11c). High displacement gradients close to the fault tips mainly reflect a 100% increase in thickness of a clay-rich interval in the relay zone between horizons 20 and 21. This thickening is accompanied by thinning and rotation of the same bed immediately outside the relay zone adjacent to segment 2.

This example of an extensional relay zone differs from the contractional relay zones presented in a number of respects. Firstly, bed rotations are less than those for a contractional relay zone of similar displacement and overlap separation. High displacement gradients at fault tips at the extensional relay zone are accommodated mainly by bed thickness changes and this difference may partly reflect the ability of layers within the deformed sequence to flow. Secondly, the fold axial traces are parallel to the fault traces for the extensional relay zone and as a consequence the fold limb length is maintained while bed rotations decrease with distance from the fault tip. This geometry is in contrast to that of contractional relay zones where limb dip is maintained but the decrease in amplitude is affected by a reduction in limb length.

4.3. Neutral relay zone

The two thrust segments shown in Fig. 12 form a neutral relay zone (Table 1) that parallels the fault slip direction and extends for an unknown distance up and down section within the Carboniferous sequence at Broadhaven. Fault segments with displacements ≤0.8 m define a relay zone with a overlap separation of ~0.75 m, which occurs between the lateral tip regions of two faults (Table 1). Within the relay zone, beds are rotated up to ~20–30° from regional bed dips; however, much of the strain is accommodated by two backthrusts (Fig.12a, c and d). In

addition, the relay zone is breached by the western thrust segment. Like the contractional and extensional relay zones, displacements on each segment decrease rapidly within the relay zone (Fig. 12e). The displacement low on the main fault segments within the relay zone is to a certain extent removed by the inclusion of throws from the backthrusts (Fig. 12e). Backthrusts oblique to bedding, which were not observed at contractional or extensional relay zones, may reflect the presence of a relatively thick sandstone bed (ca. 0.3–0.5 m) within the relay zone, which locally promotes faulting rather than folding.

5. Formation of segmented thrusts and folds

5.1. Timing of thrusting and folding

The spatial and geometric relationships between thrust segments and folds in Figs. 5–12 suggest that their origins and subsequent evolution were closely related. Here we propose that thrust segmentation occurs at low fault displacements, predating folding which takes place between the thrust segments as displacement increases. Although no means are available to determine the absolute timing of thrusting and folding, this relative timing is supported by two pieces of evidence. Firstly, complementary changes in displacements (Figs. 6–8), i.e. thrust displacement gradients of similar but opposite sign, indicate a strong interaction between structures. The smooth aggregate profiles of thrust and fold displacement for each of the examples show that thrusts and folds form part of a single geometrically (Fig. 2), and presumably kinematically, coherent structure (cf. Walsh and Watterson, 1991).

Secondly, with the exception of the lower ~4 m of the upper segment at Black Rock Quarry (Fig. 6), bedding cutoff angles with the faults change significantly (typically 30–80°) across thrusts in the region of bed rotations (Figs. 5–8). Cutoff angles in the footwall of upper thrusts are similar to those in the hanging wall of lower thrusts. The similarity of cutoff angles in the region between fault segments and the lack of folding outside the zone of fault overlap are consistent with folding occurring between existing thrust surfaces that can effectively be regarded as easy-slip surfaces along which slip accumulates during bed rotation.

The synchronous formation of thrust segments suggests that segmentation occurred at low fault displacements in one of the structural locations illustrated in Fig. 4b and c. An alternative model is one in which faulting propagated vertically and within the plane of the cross-section so that a tip-line fold formed in association with one or other of the two faults and, following fold amplification, the fold was cut by a second en échelon fault. In this sequential fault model there is no requirement for high displacement gradients on the later formed fault, which is not consistent with the examples presented. In addition, the later formed fault should have displacements that are significantly lower than the earlier formed fault and the overall structure would not show the smooth aggregate displacement profiles seen in each of the outcrop examples and which are suggestive of a kinematically coherent system. Finally, in order to produce the observed cutoff geometries with little or no folding outside the zone of overlap, this model requires that the later fault forms along the axial plane of a kink fold; the folds in the structures described do not have kink geometries. A vertical propagation and sequential fault formation model is therefore not sustainable.

It is possible to conceive of other mechanisms for the formation of the observed structures. For example, the faults may have formed in kinematic isolation to one another with late-stage bedding-parallel slip producing near alignment of faults. Such models appeal to coincidental alignment of thrusts with complementary displacement distributions and, like the sequential fault model, do not account for the displacement patterns nor the spatial relationships of the thrusts and folds observed. We believe that the model proposed here provides the simplest explanation of the field observations.

Our preferred model for the timing of thrusting and folding is, in terms of fault geometry, identical to that of Tanner (1992) for duplex formation, where pairs of bedding parallel slip surfaces effectively bound a relay zone prior to linkage by ramp formation and duplexing. The only difference between the model suggested here and that of Tanner (1992) is the angle between the faults and bedding. The model is also consistent with suggestions that rapid fault propagation is concomitant with minimal folding (Suppe and Medwedeff, 1990; Wickham, 1995).

One of the implications of a model in which thrust faults are kinematically related before the accumulation of significant displacements, is that the fault segments are more likely to have formed as elements of a single structure at the time of initiation (Fig. 4), rather than by interaction between initially isolated faults. This is particularly true where the distance to other neighboring thrusts is large in relation to the overlap separation between kinematically related thrust segments (e.g., $\times 10$), for example at Black Rock Quarry and Broadhaven 1 and 2. The thrust at Black Rock Quarry (Fig. 9) comprises three segments and also four structures interpreted to be breached relay zones, so that the fault trace initially comprised seven separate fault segments. The thrust shown in Fig. 9 is the only significant fault exposed within the quarry and it is extremely unlikely that this segmented fault trace formed by a random alignment of isolated faults. Our preferred model for the formation of this structure is that it originated as a series of segments, at the lateral tip of a propagating fault (Fig. 4).

5.2. Two-dimensional model of relay zone formation

Field examples indicate that a model for the origin of

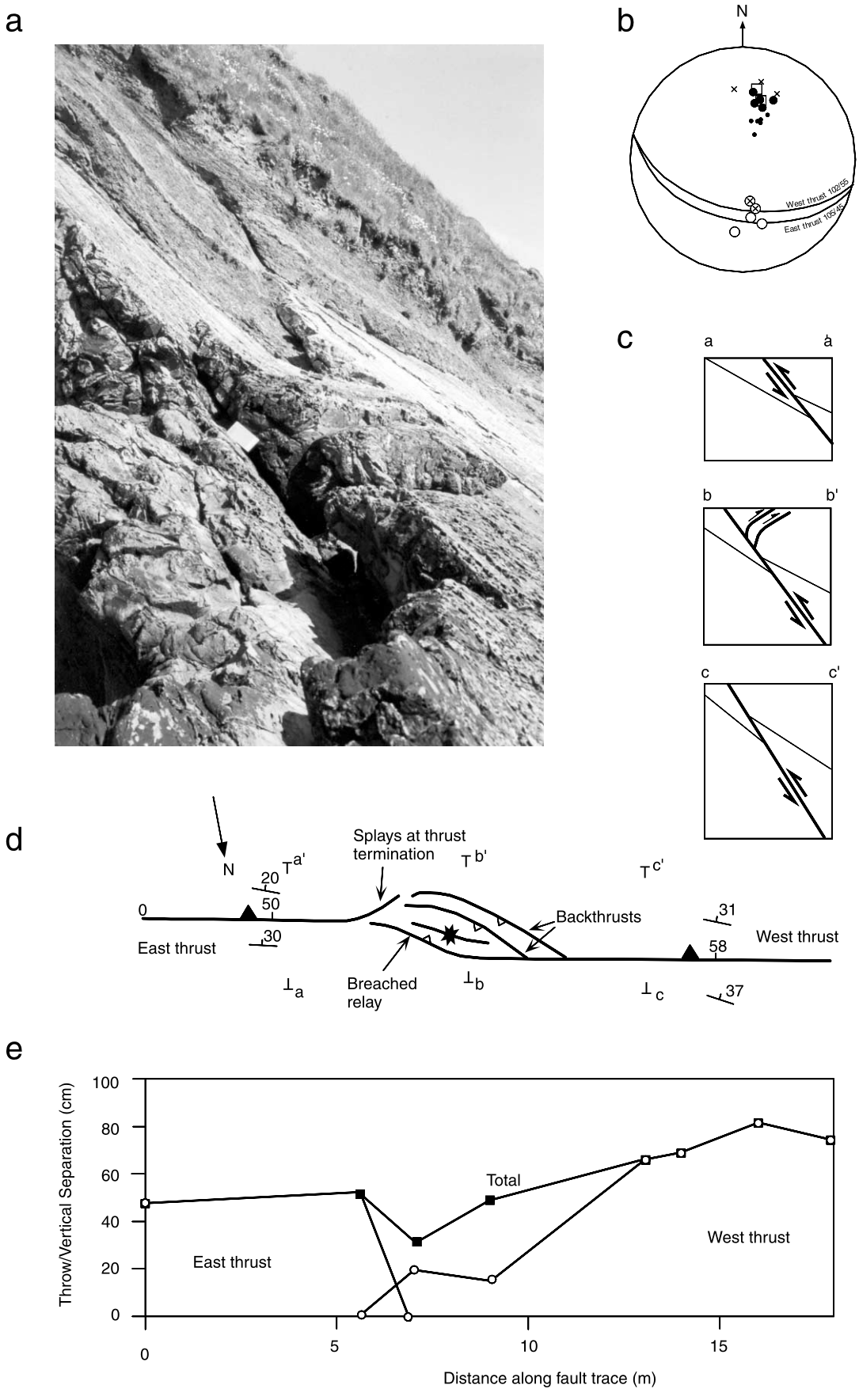
a
b
N
West thrust 102/65
East thrust 105/45
c
a
a'
b
b'
c
c'
d
N
20
Ta'
Splays at thrust
termination
Tb'
Tc'
0
50
East thrust
30
Backthrusts
31
West thrust
58
⊥a
Breached
relay
⊥b
⊥c
37
e
Throw/Vertical Separation (cm)
100
80
60
40
20
0
Total
East thrust
West thrust
0
5
10
15
Distance along fault trace (m)

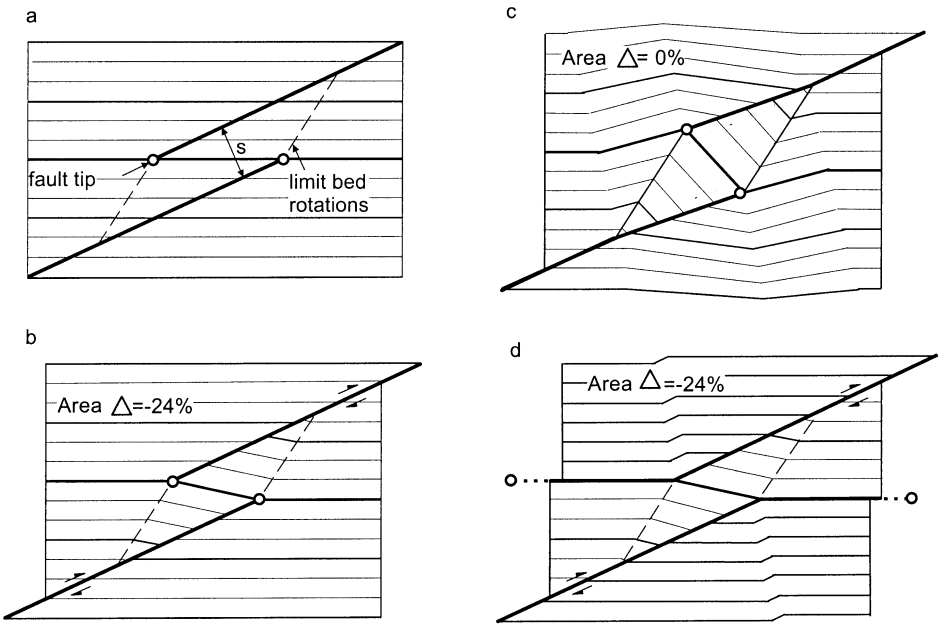

Fig. 13. Geometric model for the development of contractional thrust relay zones from an initial starting condition (a). Three variations on the model are (b) constant overlap separation (s), (c) constant area within the relay zone, and (d) constant overlap separation but incorporating bedding parallel slip. The models in (b) and (c) are shown for displacement = 0.9 m. There is an additional 0.25 m component of bedding parallel displacement in (d). The models were constructed according to the following conditions; (i) thrust segments are initially planar, inclined at 25° to bedding with overlap separation of 1 m, (ii) tip points for thrust segments were pinned at a common horizon and allowed to move relative to each other as displacement accrued, (iii) the relay fold is angular and the hinge position fixed relative to the stratigraphy, (iv) aggregate shortening is invariant across the overlap and accommodated by equal amounts of absolute footwall and hanging wall motion, (v) area is conserved outside the relay zone, and (vi) the region of overlap was deformed by inclined simple shear parallel to the thrust planes. Change in area (Area Δ) of the relay zone is given as a percentage of the initial area of the relay zone.

folds at thrust relay zones should account for the following main characteristics;

(i) Thrust segments predate folding.
(ii) Bed rotations within the relay zones increase with increasing fault displacement.
(iii) Changes in thrust and fold displacements are equal and opposite.
(iv) Significant internal deformation occurs within the relay zones, including bedding-parallel slip, small-scale thrusts and duplexes, and pressure-solution cleavage.
(v) Fold hinges are fixed relative to the stratigraphy.

These main features may be associated with;

(vi) Thrust tips that lie within a common stratigraphic interval (Figs. 6–8 and 11).
(vii) Overlap separation which is approximately constant (Figs. 6, 8 and 11) or increases slightly (Figs. 5 and 7) as displacement accumulates.
(viii) Thrust tips that become bedding parallel at the relay zone (Figs. 6 and 7).

High displacement gradients (0.17–1.0) at thrust tips (Figs. 6–8 inset displacement profiles), marked differences in bedding cutoff angles across thrusts in the region of bed rotations and the approximate coincidence of thrust tip points with fold hinges (Fig. 3; lower thrust of Figs. 6 and 8), indicate little propagation of fault tips through the sequence after the onset of folding within the relay zones. In addition, thrust tips often terminate within a common stratigraphic layer (e.g. Figs. 6–8 and 11) which suggests that anisotropy of the sedimentary sequence has a significant impact on the location of thrust segment boundaries. Collectively these data are consistent with the notion that fault surfaces form early, prior to significant displacement. During subsequent increases of finite displacement and bed rotations, thrust tips remain fixed relative to the stratigraphy and therefore, move relative to each other parallel to the direction of slip. Such a scenario would require that fold hinges are pinned at thrust tips, which often seems to be the case for thrusts (Fig. 5; lower thrust of Figs. 6 and 8) and also for normal faults where fault tips are fixed at a common bed which rotated within the relay zone (Childs et al., 1996a).

Fig. 12. Segmented Variscan thrust in interbedded sandstones and mudstones of Carboniferous age, Broadhaven, South Wales, UK. (a) Photograph looking east (notebook is 20 cm in length). (b) Equal area plot of poles to fault segments, orientation of slickenside striations and poles to bedding (refer to Fig. 8c for key to symbols). (c) Cross-sections at locations shown in map (d). (e) Fault displacement profiles. The profile of total throw includes the contribution of backthrusts not shown individually. Referred to as Broadhaven 2 in the text and Table 1.

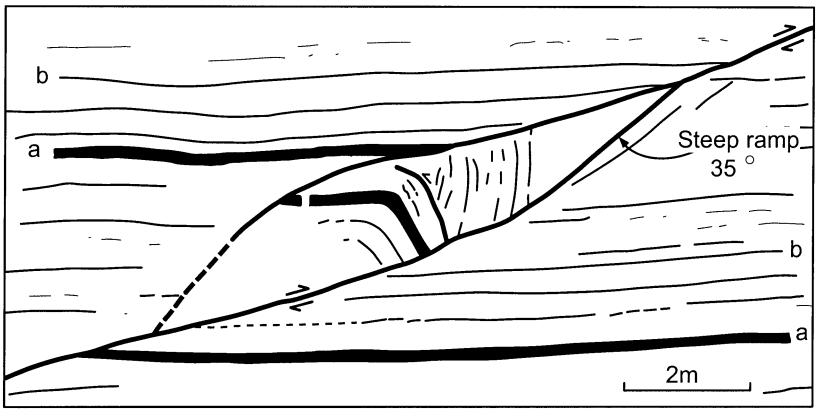

Fig. 14. Cross-section of a breached relay zone and associated bed rotations, Black Rock Quarry, South Wales. See caption of Fig. 6 for details of sequence and Fig. 9 for location.

Fig. 13 shows a simple two-dimensional (2D) geometric and kinematic model that accounts for many of the features encountered (see list above) in cross-section at contractional thrust relay zones. Extensional and neutral relay zones have not been included in Fig. 13 as we present only a single example of each and cannot be certain that these are representative. Thrust tips in the model are pinned to a common horizon but could also be fixed at different stratigraphic positions, as is the case in Fig. 5. For simplicity the folds in Fig. 13 are drawn with a kink geometry not seen in the outcrop examples. Two end-member models are considered, firstly where the volumetric strains required in the relay zone are accommodated entirely by reduction in the area of the relay zone (Fig. 13b) and secondly, the opposite case where both area and line length are conserved (Fig. 13c); the outcrop examples described will lie between these end members. A third case (Fig. 13c) is identical to the first but incorporates a component of bed parallel faulting.

The three model variations reproduce the variability of relay zone structure seen in the outcrop examples. In each case progressive formation of the relay zone structure is associated with increasing fault slip and layer rotation within the relay zone. In the first model, constrained by constant overlap separation (Fig. 13b), with progressive limb rotations and displacement accumulation, fault tips move parallel to the fault traces by a net amount equal to the finite fault displacement external to the relay zone. Fig. 13b is broadly consistent with Figs. 5–8 and shows thrust segments to be separated by an asymmetric fold, with higher cutoff angles within the thrust relay zone than external to it. As the overlap separation remained approximately constant during folding (Figs. 6 and 8), clockwise bed rotations, i.e. towards a fault-normal orientation, produce a decrease in limb length. Increasing aggregate displacement results in a decrease of the overlap length and the area of the relay zone whilst increasing the bed dips and thicknesses within the relay zone (Fig. 13a and b). Natural examples show increased bed thicknesses within the relay zone of the order predicted by the model, but despite the presence of pressure-solution cleavage in several examples (Figs. 6 and 8) insufficient data are currently available to test the validity of the significant volume loss (ca. 24%) required in Fig. 13b.

The constant area model (Fig. 13c) requires that, as displacement accrues, the overlap separation increases resulting in a divergence of fault traces, as seen in Fig. 6, and outward bending of the surrounding rocks, as seen for example in Fig. 5. The angular fold geometries depicted in Fig. 13c are not expected in natural examples. Where the relay zone bounding thrusts become bedding parallel (Fig. 13d and see Figs. 6 and 7 for natural examples), a proportion of the thrust displacement is accommodated by strains outside of the relay zone rather than being transferred across it. Bedding-parallel slip and an increase in overlap separation, both of which may occur in the example in Fig. 6, allow strains to be accommodated outside the relay zone and therefore greater thrust displacement to be attained before the relay zone is breached.

These simple models reproduce many of the features encountered in natural examples of contractional relay zones. Most natural examples of thrust relay zones will not necessarily comply with the constraints imposed in the models, such as constant overlap separation or constant area, and are likely to incorporate features of a single model. The degree to which a natural example will comply with one of the three models will depend on many factors, perhaps most importantly lithology. For example in rocks that can readily lose volume by pressure solution, the thrust relay zones are more likely to resemble the model illustrated in Fig. 13b. The proposed models are expected to be most applicable where thrust relay zones are localized by bedding anisotropy and where the fault propagation direction is mainly normal to the plane of observation. Additionally, our understanding of how thrust relay zones form will undoubtedly improve with acquisition of more field examples and with mechanical modeling.

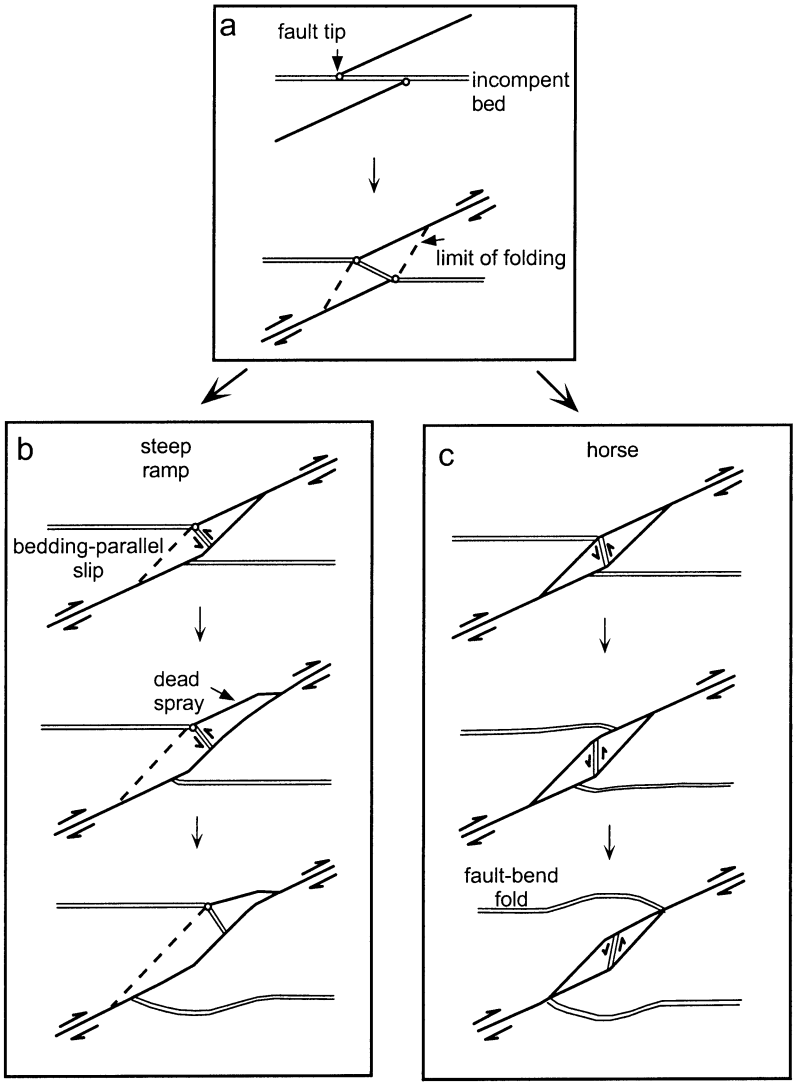

Fig. 15. (a) Schematic diagram illustrating the evolution of segmented thrusts with tips that are fixed within an incompetent bed. Fault displacement is accompanied by bed rotations within the relay zone until breaching occurs. Breaching and formation of a through-going fault may result from (b) linkage via a single steep ramp or (c) by development of two fault surfaces enclosing a horse.

6. Relay zone breaching

Relay zones oriented normal to the fault slip direction are transient features and will ultimately be breached with increasing fault displacement to produce a throughgoing fault surface (e.g. Segall and Pollard, 1980; Wesnousky, 1988; Childs et al., 1995, 1996a). Breaching occurs when the shear strain between fault segments can no longer be accommodated by continuous deformation. Where shear within a relay zone is primarily accommodated by folding and bed-parallel slip, breaching is expected to occur due to 'locking' of the fold. Breaching may be achieved by propagation of both faults to form a fault bounded horse (Figs. 14 and 15c), by propagation of one of the overlapping faults to form a connecting ramp and a 'dead' splay (Fig. 15b) or by development of a secondary fault cutting through the relay zone. The displacement at which breaching occurs is dependent on the shear modulus of rock in the relay zone, the overlap separation, the angle between mechanical layering and the fault surface, and the type of relay zone.

Rocks with a high shear modulus (e.g. granite or massive sandstone) are less likely to accommodate the high internal strains necessary to maintain the integrity of relay zones. At scales where mechanical unit thicknesses are comparable with overlap separation, lithology will exert a strong control on the internal deformation and subsequent breaching of relay zones. Where overlap separation is larger than mechanical unit thicknesses, relay zones with larger overlap separations remain intact at higher displacements than those with smaller overlap separations (Wesnousky, 1988). For example, on the large thrust at Black Rock Quarry (Figs. 6, 10, 11 and 14), which has an aggregate displacement of ~5 m and occurs within a sequence of interbedded limestones and marls, those relay zones with overlap separations

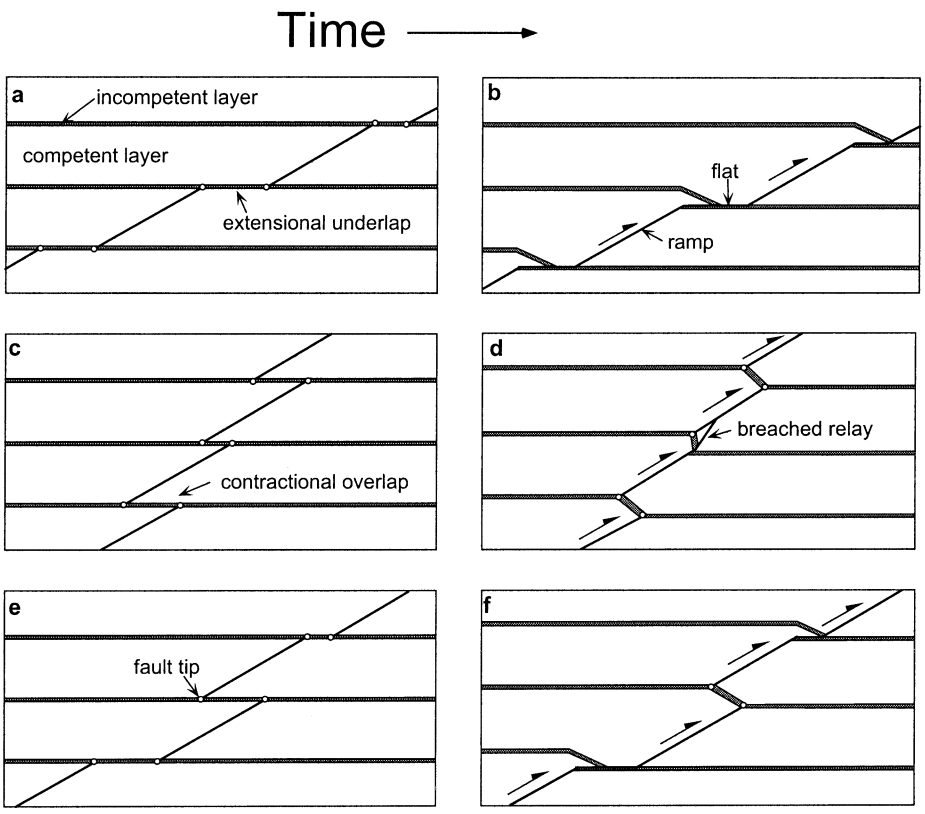

Fig. 16. Schematic diagrams showing possible initial configurations of thrust segments in sequences with strong lithological anisotropy. (a,b) Thrust comprising entirely extensional segment boundaries that may become linked by flats along incompetent layers (after Eisenstadt and De Paor, 1987). (c,d) Thrust comprising entirely contractional segment boundaries and (e,f) thrust comprising a mixture of types of segment boundaries.

of <1.3 m have been breached while those with overlap separations of >2.7 m remain intact. Therefore, the ratio of aggregate displacement to overlap separation at which relay zone failure occurred was between ~ 2 and 4. This ratio for contractional relay zones between thrusts inclined at a low angle to bedding ($<30°$) is less than ratios of $\sim 5–9$ measured for relay zones on small (throw 1–10 cm) segmented normal faults inclined at high angles (e.g. 50–80°) to bedding (Childs et al., 1996a). The tendency for thrust relay zones of a given overlap separation to be breached at lower displacements than normal faults is believed to principally reflect the higher angle between fault surfaces and mechanical layering in the latter case. These higher angles favor accommodation of strains within the relay zone by bed rotation and bed-parallel slip (Walsh et al., 1999).

The inclination of thrust segments relative to bedding is also expected to dramatically influence the breaching of extensional thrust relay zones. Where thrust tips are initially contained within a common mechanically weak layer and the thrusts dip at low angles to bedding (e.g. $<20°$), ramp-flat geometries are favored in preference to relay zones (Fig. 16a and b) and segmented faults are likely to link at low strains (Eisenstadt and De Paor, 1987). These geometries in turn promote the development of duplexes (Boyer and Elliott, 1982; Tanner, 1992). At bedding-fault angles of 50–60°, however, extensional relay zones may initially form in preference to ramp-flat geometries even where thrust tips are contained within weak layers, as is the case in Fig. 11. Measurement of breached and intact extensional relay zones at Whakataki indicate that thrust segments link at ratios of aggregate displacement to overlap separation of <1, considerably less than the values for contractional relay zones at Black Rock Quarry. This difference is partly due to bedding surfaces, which form planes of weakness, being favourably oriented to facilitate breaching of extensional relay zones, whereas bedding-parallel slip promotes flexure and the accumulation of high internal strains within contractional relay zones.

Fig. 14 shows a horse, which is defined by shallow fault traces colinear with the main fault and two steeper (35°) ramps, and comprises steeply-inclined and folded bedding and small-scale faulting. The horse is interpreted to have formed by breaching of a relay zone on two steep ramps; the ramp on the right side of the horse is coincident with a weakened fold axial surface. A similar mode of horse formation is illustrated in Fig. 15c. For the example in Fig. 14, displacement on the thrust after horse formation appears to have been small (perhaps <2 m). However, significant slip (e.g. >5 m) after breaching would result in further deformation of the horse as a lozenge within the fault zone or may produce a duplex. Duplexes are expected to

become increasingly significant with reduction in the angle between bedding and the fault surface (Tanner, 1992; Walsh et al., 1999). As an alternative to horse formation, breaching of a relay zone may occur along a single slip surface, preserving the fold as a hanging wall or footwall anticline with an associated dead splay (Fig. 15b). Subsequent slip of the hanging wall around the newly formed fault bend would result in a fold geometry that includes elements of both fault-relay zone and fault-bend folding.

A 2D model for thrust development in which non-colinear thrust segments become linked by the production of new fault trace (Fig. 16a and b) is similar to that proposed by Eisenstadt and De Paor (1987). However, instead of isolated ramps linking through bedding-parallel flats within incompetent units, our observations suggest that thrust segments that terminate at incompetent layers and initially form a contractional relay zone may become linked by steep ramps (Fig. 16c and d). A crucial difference between the alternative models is whether segment boundaries are extensional or contractional. The segmented thrust in Fig. 9 is interpreted to have included both types of relay zone, which is also typical of normal faults (Childs et al., 1996a), and may represent a more general case in which thrust-surface geometries are more complex than is predicted by either model (Fig. 16e and f). As extensional relay zones of a given overlap separation are often breached at lower displacements than contractional relay zones, we would expect the latter to be more frequently encountered.

Folding at thrust segment boundaries that have subsequently linked by relay zone breaching, may in some cases account for the presence of non tip-line folds in volumes adjacent to thrusts (e.g. Ellis and Dunlap, 1988; Wrede, 1993). Coalescence of fault segments can be inferred from the presence of bends in the fault trace, from zones of high bed rotation or strain along the fault or from displacement lows in the region of a pre-existing segment boundary (e.g. Ellis and Dunlap, 1988; Liu and Dixon, 1991; Anders and Schlische, 1994; Peacock and Zhang, 1994; Childs et al., 1995, 1996a; Lebel and Mountjoy, 1995). The absolute value of a displacement low at a relay zone will not change after breaching, as the absent displacement has been accommodated by permanent ductile strain, but will become proportionally less important with continued displacement. By analogy with relay zones on normal faults observed in vertical planes normal to bedding, thrust displacement that post-dates relay zone breaching is expected to result in progressive deformation of the former relay zone (e.g. Childs et al., 1996a). Increases in the amount of fault displacement after failure of a relay zone will make recognition of a pre-existing segment boundary increasingly difficult.

7. Discussion

The structures described here demonstrate the occurrence of relay zones that are approximately perpendicular to the thrust dip direction. Segmented thrusts of this type should occur extensively in well-bedded, mechanically heterogeneous sequences but have not been widely reported in the literature. We believe that there are three principal reasons for the apparent lack of these segmented thrust and fold structures in mechanically anisotropic sequences. Firstly, contractional and extensional segment boundaries are best observed in well exposed sections oriented at a high angle to fault strike. For small thrusts (e.g. displacement <5 m) segment boundaries could conceivably be exposed within a single outcrop. For larger displacement thrusts, the preservation potential of small overlap separation relay zones is reduced and progressively larger exposures would be required to correctly interpret intact relay zones. For example, using a value of three for the ratio of displacement to overlap separation at the point of relay zone breaching, a section of at least $\sim 200 \times 200$ m would be necessary to identify the minimum sized relay zone on a thrust with 500 m displacement. The use of seismic reflection profiles may help to identify the presence of thrust segmentation but it is unlikely that the steeply-inclined beds between the faults would be well imaged. Secondly, intact relay zones are expected to be most common where strains are low; as strains increase, duplexes, thrust ramps and bedding-parallel detachments will become more significant (e.g. Boyer and Elliott, 1982; Eisenstadt and De Paor, 1987; Tanner, 1992). Thrust data are often derived from regions of high strain (e.g. Canadian Rockies) where initially segmented faults are likely to have subsequently linked. Thirdly, there is an extensive literature on folds that form beyond the propagating tip-line of thrust surfaces (e.g. Boyer, 1986; Mitra et al., 1988; Chester and Chester, 1990; Suppe and Medwedeff, 1990) and folds formed above the lower thrust segment in contractional relay zones could be interpreted in this manner. This is particularly likely where the upper thrust has been eroded or is poorly exposed. Therefore, in some cases folds at contractional thrust relay zones could have been misidentified as leading-edge folds and consequently their importance may be underestimated.

The location and orientation of relay zones is strongly influenced by the position of mechanically weak beds and relay zones oriented parallel to the thrust/bedding intersection (e.g. Figs. 6, 8 and 12) should comprise a large proportion of the total population of segment boundaries. For example, close spatial relationships between folds and incompetent beds were observed at the Nant Helen open pit (outside of the area in Fig. 5) where thrusts passed downwards into folds at the incompetent lower coal seams. These folds are of limited vertical extent and mine workings below the incompetent seams indicate that here the thrusts again become discrete structures. In such cases the resulting low in thrust displacements reflects a change in the style of deformation along a single structure rather than termination of the structure.

Assuming that the region of nucleation of a fault lies at or close to its point of maximum displacement, lines within the fault surface and radiating from this point indicate fault propagation directions (Watterson, 1986). Therefore, cross-sections through faults, with the exception of those through the point of maximum displacement, will contain a fault trace formed with a component of out-of-plane propagation. Given that the aspect ratios of thrust surfaces are typically >3 and elongate in the slip normal direction (Gillespie, 1991), the component of lateral propagation will generally exceed that of vertical propagation. Arguments for the propagation and evolution of thrusts based on cross-sectional data must therefore take account of lateral propagation.

8. Conclusions

1. Segmented thrusts may form in well-bedded, mechanically heterogeneous, sequences. Thrust segments at contractional relay zones are separated by asymmetric folds with steep to moderate bed dips of $\sim$30–75° between the faults and shallow bed dips outside the relay zone. Folds verge in the direction of hanging wall motion relative to the footwall, with the steeper limb of the fold often defining a parallelogram-shaped region between thrusts.
2. Fault displacements decrease rapidly at relay zones and are matched by a complementary increase in fold amplitude. High displacement gradients at thrust tips are mainly accommodated by bed rotations within contractional relay zones.
3. Thrust relay zones form after minimal fault displacement and folds grow between thrust segments as they accrue displacement. Bed rotations within relay zones allow aggregate displacement to be maintained across the segment boundary and accommodate the transfer of displacements between thrust segments. During folding, thrust tips may remain fixed relative to the stratigraphy and therefore move relative to each other parallel to the direction of slip.
4. Relay zones become breached with increasing displacement. Contractional relay zones can sustain higher displacements before breaching than extensional relay zones, while increases in the bedding-thrust angle and overlap separation also promote longevity of segmented thrusts.

Acknowledgements

We wish to thank Rodney Gayer, Volke Wrede and members of the Fault Analysis Group for helpful discussions on aspects of this work and Rodney Gayer for his supervision of P.A. Gillespie's PhD at Cardiff, on which part of this paper is based. Thanks also to Tanya Hathaway for supplying photographs of Black Rock Quarry and for discussion in the field and to Elizabeth Sweeney for helping to prepare the final manuscript. D.A. Spratt and an anonymous reviewer are thanked for their very helpful reviews and we are particularly grateful to Mark Fischer whose comments led to a significant improvement of the manuscript. Geoff Rait, Volke Wrede, and Jim Evans are thanked for their reviews of earlier versions of the manuscript.

References

Anders, M.H., Schlische, R.W., 1994. Overlapping faults, intrabasin highs and the growth of normal faults. Journal of Geology 102, 165–180.

Aydin, A., 1988. Discontinuities along thrust faults and the cleavage duplexes. Geological Society of America 222, 223–233.

Aydin, A., Nur, A., 1985. The types and role of stepovers in strike-slip tectonics. In: Biddle, K.T., Christie-Blick, N. (Eds.). Strike Slip Deformation, Basin Formation and Sedimentation, pp. 35–44 Special Publication of the Society of Economic Paleontologists and Mineralogists 37.

Barnett, J.A.M., Mortimer, J., Rippon, J.H., Walsh, J.J., Watterson, J., 1987. Displacement geometry in the volume containing a single normal fault. American Association of Petroleum Geologists Bulletin 71, 925–937.

Boyer, S.E., 1986. Styles of folding within thrust sheets: examples from the Appalachians and the Rocky Mountains of the USA and Canada. Journal of Structural Geology 8, 325–339.

Boyer, S.E., Elliott, D., 1982. Thrust systems. American Association of Petroleum Geologists Bulletin 66, 1196–1230.

Cartwright, J.A., Trudgill, B., Mansfield, C.S., 1995. Fault growth by segment linkage: an explanation for scatter in maximum displacement and trace length data from the Canyonlands Grabens of S.E. Utah. Journal of Structural Geology 17, 1319–1326.

Chapman, T.J., Williams, G.D., 1984. Displacement-distance methods in the analysis of fold-thrust structures and linked fault systems. Journal of the Geological Society of London 141, 121–128.

Chester, J., Chester, F., 1990. Fault propagation folds above thrusts with constant dip. Journal of Structural Geology 12, 903–910.

Childs, C., Watterson, J., Walsh, J.J., 1995. Fault overlap zones within developing normal fault systems. Journal of the Geological Society of London 152, 535–549.

Childs, C., Nicol, A., Walsh, J.J., Watterson, J., 1996a. Growth of vertically segmented normal faults. Journal of Structural Geology 18, 1389–1397.

Childs, C., Watterson, J., Walsh, J.J., 1996b. A model for the structure and development of fault zones. Journal of the Geological Society of London 153, 337–340.

Dahlstrom, C.D.A., 1969. Balanced cross-sections. Canadian Journal of Earth Sciences 6, 743–757.

Dahlstrom, C.D.A., 1970. Structural geology in the eastern margin of the Canadian Rocky Mountains. Bulletin of Canadian Petroleum Geologists 18, 332–406.

Eisenstadt, G., De Paor, D.G., 1987. Alternative model of thrust-fault propagation. Geology 15, 630–633.

Elliott, D., 1976. The motion of thrust sheets. Journal of Geophysical Research 81, 949–963.

Ellis, M.A., Dunlap, W.J., 1988. Displacement variation along thrust faults: implications for the development of large faults. Journal of Structural Geology 10, 183–192.

Ferril, D.A., Stamatakos, J.A., Sims, D., 1999. Normal fault corrugation: implications for growth and seismicity of active normal faults. Journal of Structural Geology 21, 1027–1038.

Gardner, D.A.C., Spang, J.H., 1973. Model studies of the displacement transfer associated with overthrust faulting. Bulletin of Canadian Petroleum Geology 21, 534–552.

Gillespie, P.A., 1991. Structural analysis of faults and folds with examples from the South Wales Coalfield and the Ruhr Coalfield. Ph.D. thesis, University of Wales.

Griffiths, P.S., 1980. Box-fault systems and ramps: atypical associations of structures from the eastern shoulder of the Kenya Rift. Geological Magazine 117, 579–586.

Gupta, A., Scholz, C.H., 2000. A model of normal fault interaction based on observations and theory. Journal Structural Geology 22, 865–879.

Hathaway, T.M., Gayer, R.A., 1996. Thrust-related permeability in the South Wales Coalfield. In: Gayer, R., Harris, I. (Eds.). Coalbed Methane and Coal Geology, pp. 121–132 Geological Society Special Publication 97.

Hedlund, C.A., 1997. Fault-propagation, ductile strain, and displacament-distance relationships. Journal of Structural Geology 19, 243–248.

House, W.M., Gray, D.R., 1982. Displacement transfer at thrust terminations in southern Appalachians — Saltville Thrust as example. American Association of Petroleum Geologists Bulletin 66, 830–842.

Huggins, P., Watterson, J., Walsh, J.J., Childs, C., 1995. Relay zone geometry and displacement transfer between normal faults recorded in coal-mine plans. Journal of Structural Geology 17, 1741–1755.

Kattenhorn, S.A., McConnell, D.A., 1994. Analysis of outcrop-scale fault-related folds, Eagle Rock, Virginia. Southeastern Geology 34, 79–88.

Larsen, P.H., 1988. Relay structures in a Lower Permian basement-involved extension system, East Greenland. Journal of Structural Geology 10, 3–8.

Lebel, N., Mountjoy, E.W., 1995. Numerical modelling of propagation and overlap of thrust faults, with application to the thrust-fold belt of central Alberta. Journal of Structural Geology 17, 631–646.

Liu, S., Dixon, J.M., 1991. Centrifuge modelling of thrust faulting: structural variation along strike in fold-thrust belts. Tectonophysics 188, 39–62.

McConnell, D.A., Kattenhorn, S.A., Benner, L.M., 1997. Distribution of fault slip in outcrop-scale fault related folds, Appalachian Mountains. Journal of Structural Geology 19, 257–267.

Mitra, G., Hull, J.M., Yonkee, W., Protzman, G.M., 1988. Comparison of mesoscopic and microscopic deformation styles in the Idaho–Wyoming thrust belt and Rocky Mountain foreland. In: Schmidt, C.J., Perry Jr, W.J. (Eds.). Interaction of the Rocky Mountain Foreland and the Cordilleran Thrust Belt, pp. 119–141 Memoirs of the Geological Society of America 171.

Morley, C.K., Nelson, R.A., Patton, T.L., Munn, S.G., 1990. Transfer zones in the East African rift System and their relevance to hydrocarbon exploration in rifts. American Association of Petroleum Geologists Bulletin 74, 1234–1253.

Muraoka, H., Kamata, H., 1983. Displacement distribution along normal fault traces. Journal of Structural Geology 5, 483–495.

Peacock, D.C.P., 1990. Displacements, segment linkage and relay ramps in normal fault zones. Ph.D. thesis, University of Southampton.

Peacock, D.C.P., 1991. Displacements and segment linkage in strike-slip fault zones. Journal of Structural Geology 13, 1025–1075.

Peacock, D.C.P., Sanderson, D.J., 1991. Displacements, segment linkage and relay ramps in normal fault zones. Journal of Structural Geology 13, 721–733.

Peacock, D.C.P., Sanderson, D.J., 1994. Geometry and development of relay ramps in normal fault systems. American Association of Petroleum Geologists Bulletin 78, 147–165.

Peacock, D.C.P., Zhang, X., 1994. Field examples and numerical modelling of oversteps and bends along normal faults in cross-section. Tectonophysics 234, 147–167.

Scholz, C.H., 1990. The mechanics of earthquakes and faulting. Cambridge University Press.

Segall, P., Pollard, D.D., 1980. Mechanics of discontinuous faults. Journal of Geophysical Research 85, 4337–4350.

Stewart, I.S., Hancock, P.L., 1991. Scales of structural heterogeneity with neotectonic normal fault zones in the Aegean region. Journal of Structural Geology 13, 191–204.

Suppe, J., Medwedeff, D.A., 1990. Geometry and kinematics of fault-propagation folding. Eclogae Geologicae Helvetiae 83, 409–454.

Tanner, P.W., 1992. Morphology and geometry of duplexes formed during flexural-slip folding. Journal of Structural Geology 14, 1173–1192.

Trudgill, B., Cartwright, J., 1994. Relay-ramp forms and normal fault linkages, Canyonlands National Park, Utah. Bulletin of the Geological Society of America 106, 1143–1157.

Walsh, J.J., Watterson, J., 1991. Geometric and kinematic coherence and scale effects in normal fault systems. In: Roberts, A.M., Yielding, G., Freeman, B. (Eds.). The Geometry of Normal Faults, pp. 193–203 Geological Society Special Publication 6.

Walsh, J.J., Watterson, J., Bailey, W., Childs, C., 1999. Fault relays, bends and branch-lines. Journal of Structural Geology 21, 1019–1026.

Watterson, J., 1986. Fault dimensions, displacements and growth. Pure and Applied Geophysics 124, 365–373.

Wesnousky, S.G., 1988. Seismological and structural evolution of strike-slip faults. Nature 335, 340–343.

Wickham, J., 1995. Fault displacement-gradient folds and the structure at Lost Hills, California (USA). Journal of Structural Geology 17, 1293–1302.

Williams, G., Chapman, T., 1983. Strains developed in the hanging walls of thrusts due to their slip/propagation rate: a dislocation model. Journal of Structural Geology 5, 563–571.

Woodcock, N.H., Fischer, M., 1986. Strike-slip duplexes. Journal of Structural Geology 8, 725–735.

Wrede, V., 1993. Some aspects of interactivity between folding and thrusting in the Ruhr Carboniferous. In: Gayer, R.A., Greiling, R.O., Vogel, A. (Eds.). The Rhenohercynian and Subvariscan Fold Belts. Earth Evolution Science, Vieweg, pp. 241–268.